

THREE-DIMENSIONAL SIMULATION OF LIQUID FLOW ON A SIEVE TRAY UNDER DIFFERENT INCLINATIONS

Zhang Ping^{1,2*}, Jin Dan³, Meng Huibo³ and Wu Jianhua³

¹School of Chemical Engineering and Technology, Tianjin University, Tianjin, 300072, China.

²College of Mechanical Engineering, Shenyang University of Chemical

Technology, Shenyang, 110142, China.

Mobil Phone: 86-015840013416

E-mail: zhangping19_77@163.com

³School of Energy and Power Engineering, Shenyang University of Chemical Technology, Shenyang, 110142, China.

(Submitted: October 17, 2013 ; Revised: February 17, 2014 ; Accepted: February 22, 2014)

Abstract - The fluid state on a sieve tray will change when the towers tilt under wind loads. A computational fluid dynamics (CFD) model was used to predict the flow patterns and hydraulics on the tray under different inclinations. The gas and liquid phases are modelled with the volume-of-fluid (VOF) framework as two immiscible phases. Several three-dimensional transient simulations were carried out for a 0.38m diameter tray with varying liquid weir loads and inclined angles. The clear liquid height determined from these simulations is in reasonable agreement with experimental measurements carried out for air-water in a round tray of the same dimensions. The simulation results show that, compared with the horizontal tray, the circulation area is bigger when the liquid flow and inclination direction of the tray are the same, but when they are opposite the circulation area is smaller. The percentage of circulation area to the tray area can obviously be decreased, along with increasing liquid weir loads. It is concluded that CFD can be used for the prediction of liquid flow on sieve trays under different inclinations

Keywords: Inclination; Volume of Fluid (VOF) method; Tray; Clear liquid height.

INTRODUCTION

The tray column has been widely used in many chemical separation processes, especially distillation, due to its simple structure, lower cost, and easier enlargement compared with other type towers (Sun *et al.*, 2011). The performance of a large distillation column always suffers from a loss of separation ability due to maldistributed or abnormal flow of the liquid phase on the tray. For example, liquid phase circulation, which frequently occurs on a tray, may cause a serious reduction in the Murphree tray efficiency (Yu *et al.*, 1999). Therefore, to accurately predict the tray efficiency, the hydrodynamics of non-uniform flow

on the tray must be considered (Bell and Solari, 1974; Yu *et al.*, 1983). Because the ratio of tower height to diameter is large and the shell of the tower is thin, a greater deflection will occur when the tower is subjected to wind loads. Gas-liquid mass transfer is inhomogeneous due to the deflection, which leads to the decline of tower efficiency (Zhang *et al.*, 2011).

The tower will tilt and the liquid on the tray will be non-uniform when it is subjected to wind loads. The bubble distribution will gradually increase from the thin region to the thick region and gas will move through the thick liquid layer with a higher speed and the thin liquid layer with a lower speed. The gas flow is uneven due to the gas channeling (Kister and

*To whom correspondence should be addressed

Larson, 1992; Huang *et al.*, 1996) and gas-liquid contact is insufficient. The thick side is prone to weeping and to entrainment for the thin one (Liu and Lu, 1990), which seriously affect tray efficiency. The poor distribution of weeping from a distillation tray and its effect on tray efficiency were discussed by Zeng (2002). The extent of the Murphree tray efficiency drop depended chiefly on the degree of inadequate distribution and the percentage of weeping.

Recently, advances and interest in the use of CFD techniques have been used for the study of fluid dynamics in process equipment. Zhang and Yu (1994) employed the k- ϵ two-equations model of CFD for simulating the liquid phase flow pattern on a sieve tray. A single-pass sieve distillation tray was simulated with a three-dimensional CFD program with the k- ϵ turbulence model and a source term S_{M_i} was formulated in the Navier-Stokes equations to represent the interfacial momentum transfer (Liu and Liu, 2002). The volume-of-fluid (VOF) technique can be used for *a priori* determination of the morphology and rise characteristics of single bubbles rising in a liquid (Krishna *et al.*, 1999). A three-dimensional two-phase flow model based on the VOF method for simulating the hydrodynamics and mass-transfer behavior in a typical representative unit of the structured packing is developed (Chen *et al.*, 2009). Some prior research on gas-liquid flow on a distillation tray using CFD techniques can be mentioned (Buwa and Ranade, 2003; Gesit *et al.*, 2003).

In this paper a three-dimensional transient CFD model is developed, within the two-phase VOF framework, to describe the hydrodynamics on a 0.38 m diameter sieve tray under different inclinations. Simulations have been carried out with varying liquid weir loads and incline angles. The results of the simulation are compared with experimental data generated for the air-water column. The objective of this work is to examine the extent to which CFD models can be used as a research tool for the trays under different inclinations.

EXPERIMENTAL SET-UP

The experimental set-up, shown in Figure 1, consists of four circular plates without holes and a liquid distribution device. The parameters of the tray and experiment are given in Table 1. The first plate is not the experimental plate but rather the two middle plates in order to eliminate the non-uniformity of water. The liquid from the water tank (8) was fed to the plate (4) by a liquid pump (1). The liquid flow rate was measured by a calibrated liquid flowmeter (3). By the adjustment of screw (7), the inclination angle of the tray could be adjusted. For a specified set of working conditions, the clear liquid height on the tray (5) was measured with two graduated scales attached to the wall of the inlet and outlet weir, respectively.

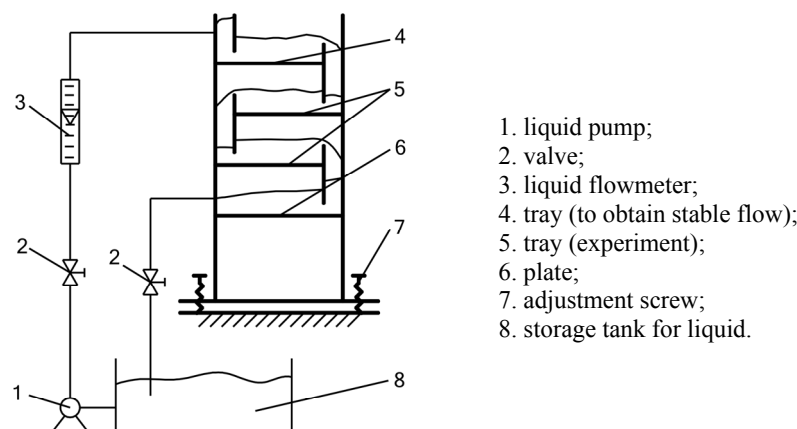


Figure 1: Experimental apparatus

Table 1: The parameters of tray and experiment.

parameters	value	parameters	value
tray diameter/m	0.38	outlet weir length/m	0.257
height of inlet/m	0.03	height of out weir/m	0.04
liquid load/m ³ ·h ⁻¹	0.5 ~ 2.5	inclination of tray/°	0 ~ 4

CFD MODEL DEVELOPMENTS

Mechanical Model

The tower will incline due to the wind loads when it is in operation. Liquid flow distribution on the tray is shown in Figure 2 and indicates that the liquid flow direction and tilt direction of the tower are the same for the i th tray and contrary for the $(i-1)$ th tray. θ_i is the inclination angle of the i th tray.

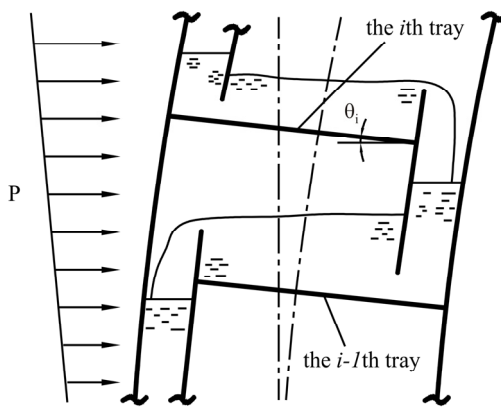


Figure 2: Liquid flow distributions on the tray

Mathematical Model

The VOF method is an effective approach for tracking the free surface. The fields of all variables and properties are shared by all the phases. Thus, the variables and properties in any given cell are either pure representatives of one of the phases, or representative of a mixture of all the phases, depending upon the volume fraction values. The tracking of the interface between the phases is accomplished by the solution of a continuity equation for the volume fraction of one (or more) of the phases (Hong, 2003). For the q th phase, the equation can be written

$$\frac{\partial \alpha_q}{\partial t} + \frac{\partial(u_i \alpha_q)}{\partial x_i} = 0 \quad (1)$$

In each control volume, the volume fraction sum of all phases is equal to 1.

$$\sum_{q=1}^n \alpha_q = 1 \quad (2)$$

Mass and momentum conservation equations are given by:

$$\frac{\partial \rho}{\partial t} + \frac{\partial(\rho u_i)}{\partial x_i} = 0 \quad (3)$$

$$\frac{\partial(\rho u_i)}{\partial t} + \frac{\partial(\rho u_i u_j)}{\partial x_j} = - \frac{\partial p}{\partial x_i} + \frac{\partial}{\partial x_j} (\mu \frac{\partial u_i}{\partial x_j}) + \mathbf{F} \quad (4)$$

The momentum conservation equation is enclosed by means of the k- ε mode1.

The transport equation for k is:

$$\frac{\partial(\rho k)}{\partial t} + \frac{\partial(\rho u_i k)}{\partial x_i} = \frac{\partial}{\partial x_i} \left[\left(\mu + \frac{\mu_e}{\sigma_k} \right) \frac{\partial k}{\partial x_i} \right] + G - \rho \varepsilon \quad (5)$$

The transport equation for ε is:

$$\begin{aligned} \frac{\partial(\rho \varepsilon)}{\partial t} + \frac{\partial(\rho u_i \varepsilon)}{\partial x_i} = & \frac{\partial}{\partial x_i} \left[\left(\mu + \frac{\mu_e}{\sigma_\varepsilon} \right) \frac{\partial \varepsilon}{\partial x_i} \right] \\ & + (C_1 G - C_2 \varepsilon) \frac{\varepsilon}{k} \end{aligned} \quad (6)$$

where, μ_e is the turbulent viscosity:

$$\mu_e = \rho C_\mu \frac{k^2}{\varepsilon} \quad (7)$$

$$G = \mu_e \left(\frac{\partial u_i}{\partial x_j} + \frac{\partial u_j}{\partial x_i} \right) \frac{\partial u_i}{\partial x_j} \quad (8)$$

In the VOF framework, a single momentum equation is solved throughout the domain, and the resulting velocity field is shared among the phases. The equation, as originally stated, depends on the volume fractions of all phases through ρ and μ , as shown in Equation (9). \mathbf{F} is body force on the control element and only acted upon by gravity.

$$\rho = \sum_{q=1}^n \alpha_q \rho_q, \mu = \sum_{q=1}^n \alpha_q \mu_q \quad (9)$$

where the constants are taken from the literature (Launder, 1989), as follows:

$$C_1 = 1.44, C_2 = 1.92, C_\mu = 0.09, \sigma_k = 1.0, \sigma_\varepsilon = 1.3$$

The coordinate system of the i th tray is shown in Figure 3. The dimensions of the computational space are the same as those in the experiment. The direction of liquid flow and the weir length are defined as x and y , respectively. The vertical direction is z .

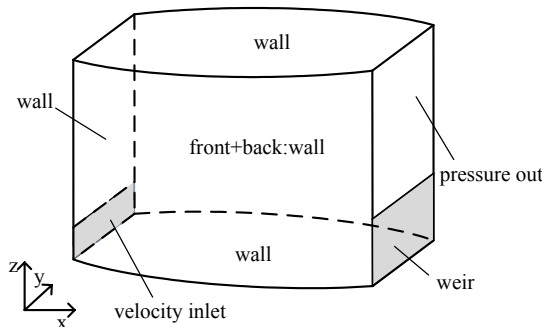


Figure 3: Computational space used in the CFD simulations

A commercial CFD package FLUENT was used to solve the equations of continuity and momentum for the two-fluid mixture. There is a finite volume solver in this package, using body-fitted grids. Grid cells of 5 mm size are used in the x -, y - and z -directions based on the experience gained in the modelling of gas-liquid bubble columns operating in the churn-turbulent regime (Krishna *et al.*, 1999; Van Baten and Krishna, 2000). The chosen grid size of 5 mm is smaller than the smallest grid used in an earlier study (Hirt and Nichols, 1981), where the grid convergence was satisfied. The boundary conditions and simulation parameters are shown in Table 2.

Table 2: The boundary conditions and simulation parameters.

content	parameters	content	parameters
liquid inlet	velocity-inlet	liquid outlet	pressure-out
gas outlet	pressure-out	liquid load per unit weir length / $\text{m}^3 \cdot \text{s}^{-1} \cdot \text{m}^{-1}$	1.08, 1.62, 2.16, 2.7
inclination angle/ $^\circ$	0, 1, 2, 3, 4	time increment /s	$10^{-4} \sim 10^{-3}$

Air and water were used as the gas and liquid phases, respectively. At the start of a simulation, the tray configuration shown in Figure 3 is filled with gas phase only. A shorter time-step was set to obtain a better simulation result (Tao, 2008). The step size can then be increased when there is a good convergence in the simulation. The time increment used in the simulations was from 10^{-4} s to 10^{-3} s. The pressure-velocity coupling was obtained using the PISO algorithm. During the simulation, the volume fraction of the liquid phase in the gas-liquid dispersion in the system was monitored. A transient simulation was supposed to converge whenever there was no appreciable change with time of the volume fraction of the liquid. Although many of the simulations were

inherently transient, an averaged parameter, the volume fraction of the liquid, can be obtained, as seen in Figure 4. Typically, the steady state is achieved in about 10 s from the start of liquid flow. It took about 2 days to simulate 20 s of an inclination tray. For obtaining the clear liquid height, the parameter values are averaged over a sufficiently long period in which the volume fraction of the liquid phase remains steady.

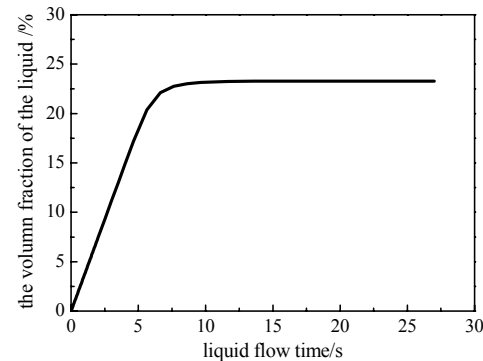


Figure 4: Changing curve of flow time with volume fraction

$$(h_w=40 \text{ mm}, Q_L/l_w = 2.7 \times 10^{-3} \text{ m}^3 \cdot \text{s}^{-1} \cdot \text{m}^{-1}, \theta=2^\circ)$$

RESULTS AND ANALYSIS OF THE SIMULATION

Simulation Results

The flow field of a 1.2m diameter tray was made by using a tracer, and the results show that there is the district of the main flow and circulation flow (Porter *et al.*, 1972). The circulation flow is reconstructed in our simulation. The fraction of circulation area of the tray is defined by Equation (10).

$$T\% = \frac{N_{-x}}{N} \quad (10)$$

The liquid velocity distribution in $z=0.02$ m is shown in Figure 5. The simulation results for the i th tray, with the same direction between the liquid flow and the tilt of the column plate, are shown in Figure 5(a). The simulation results for the $(i-1)^{\text{th}}$ tray are shown in Figure 5(c), with the opposite direction between the liquid flow and the tilt of the column plate. There is no inclination in Figure 5(b) and the area of liquid circulation lies in the tray center along the x direction. The circulation zone center biases the outlet weir in Figure 5(a) and the fraction of

circulation area is maximum in 3 cases, but the circumfluence center is towards the inlet and the fraction of circulation area is minimum in the 3 cases in Figure 5(c).

Figure 6 presents the flow field distribution of the tray in the $z=0.02$ m plane with inclinations of 2° and

4° , respectively. When the tilt of tray and the liquid flow have the same direction, with increasing inclination of the tray, the area of circulation increases. When the direction is opposite, the area of circulation will show a decreasing trend with increasing inclination of the tray.

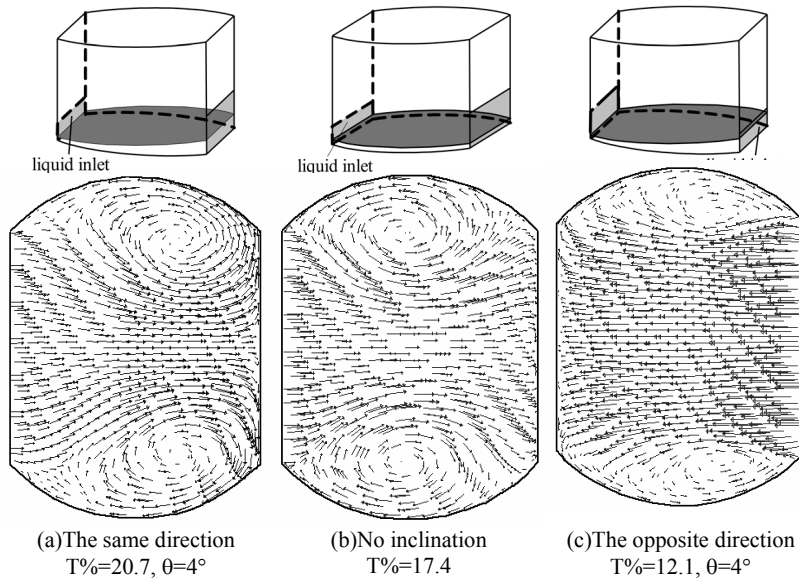


Figure 5: Liquid velocity distribution along the z direction
($h_w=40$ mm, $Q_L/l_W=1.08\times 10^{-3}$ $\text{m}^3\cdot\text{s}^{-1}\cdot\text{m}^{-1}$, $z=0.02$ m)

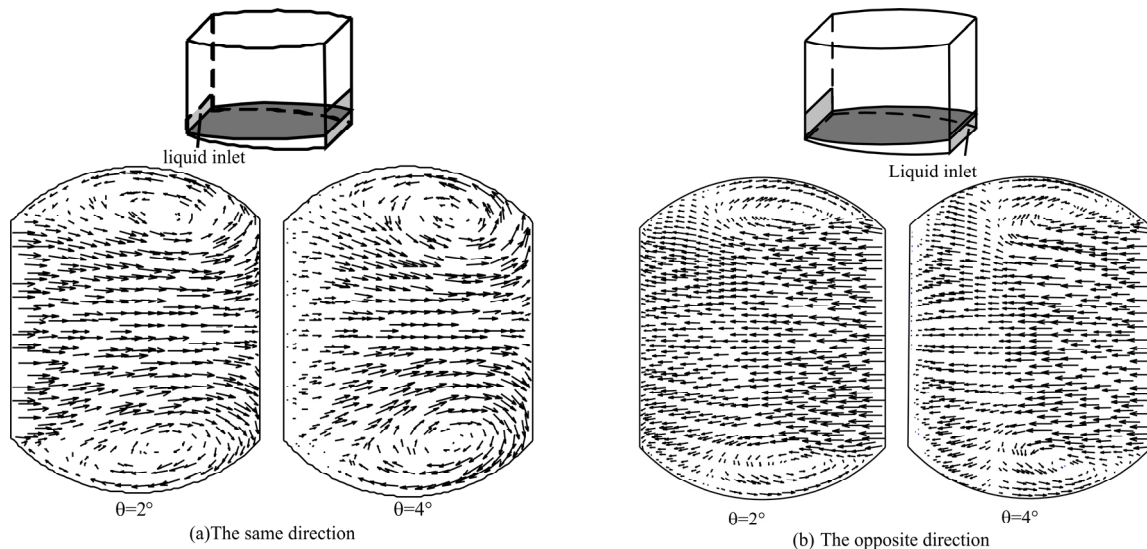


Figure 6: Flow field distribution along the z direction under different inclination
($h_w=40$ mm, $Q_L/l_W=2.7\times 10^{-3}$ $\text{m}^3\cdot\text{s}^{-1}\cdot\text{m}^{-1}$, $z=0.02$ m)

The variation of the circulation area with inclination angle is given in Figure 7. The percentages of circulation from the simulations are obtained after averaging 10 s of flow time once quasi-steady-state conditions were established.

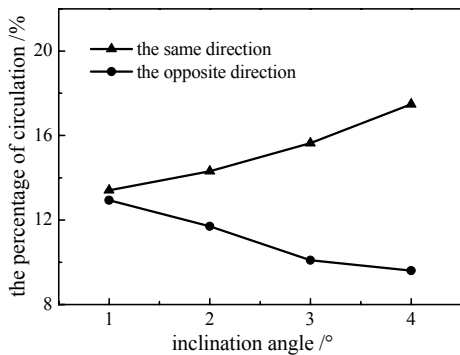


Figure 7: The fraction of circulation as a function of inclination angle

$$(h_w=40 \text{ mm}, Q_L/l_w=2.7 \times 10^{-3} \text{ m}^3 \cdot \text{s}^{-1} \cdot \text{m}^{-1}, z=0.02 \text{ m})$$

The percentage of circulation area on the tray in the z direction is shown in Figure 8. The percentages of circulation from the simulations are obtained after averaging 10 s of flow time once quasi-steady-state conditions were established. The circulation area tends to increase gradually from $z=0.02 \text{ m}$ to $z=0.03 \text{ m}$, especially for $z=0.03 \text{ m}$. The increase in rate from $z=0.03 \text{ m}$ to $z=0.04 \text{ m}$ is twice that from $z=0.02 \text{ m}$ to $z=0.03 \text{ m}$. It can be attributed to the existence of a diffuse interface from $z=0.03 \text{ m}$ to $z=0.04 \text{ m}$.

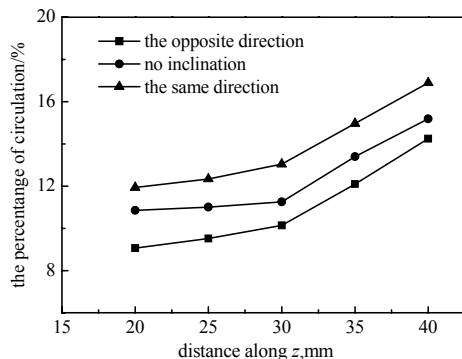


Figure 8: The fraction of circulation along the z direction

$$(h_w=40 \text{ mm}, Q_L/l_w=2.16 \times 10^{-3} \text{ m}^3 \cdot \text{s}^{-1} \cdot \text{m}^{-1}, \theta=2^\circ)$$

As can be seen from Figure 9, independent of whether the liquid flow and inclination of tray have the opposite or the same direction, the percentage of

circulation area decreases as the liquid weir loads increase, although that of the same direction decreased more rapidly. The circulation percentages from the simulations were obtained after averaging 10 s of flow time once quasi-steady-state conditions were established. The liquid acquires a greater momentum in the primary flow direction with increasing liquid weir load, so the circulation areas are reduced.

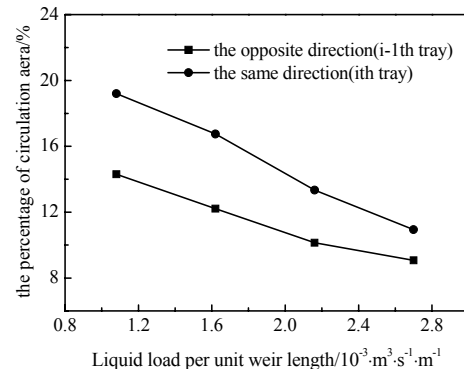


Figure 9: The fraction of circulation as a function of the liquid weir load

$$(h_w=40 \text{ mm}, z=0.02 \text{ m}, \theta=2^\circ)$$

CFD Simulations vs. Experiments

The comparisons for the clear liquid height with varying liquid weir loads between the experimental data, the simulation results from CFD, and the Francis formula, Equation (11), are shown in Figure 10.

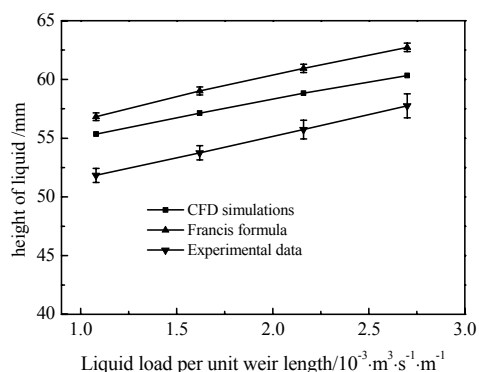
$$h_L = h_w + \frac{2.84}{1000} E \left(\frac{Q_L}{l_w} \right)^{\frac{2}{3}} \quad (11)$$

The value of E in Equation (11) is determined by Equation (12):

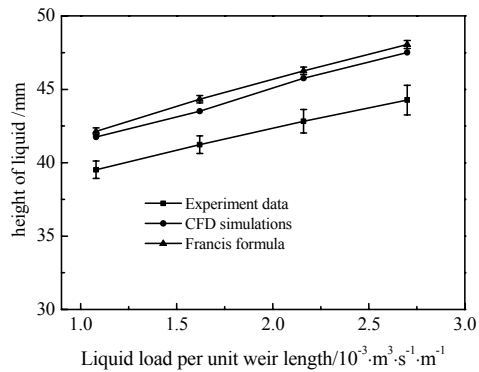
$$E = 1 + [0.00012 - 0.00386 \ln(\frac{l_w}{D})] \frac{Q_L}{l_w^{2.5}} \quad (12)$$

The error of the Francis equation is 0.756% with Equation (12) (Wang, 1990). The values of the liquid height from the simulations were obtained after averaging 10 s of flow time interval once quasi-steady state conditions were established. The results from Francis formula agree with CFD simulations perfectly. But the experimental results are lower than those two approaches. In the present experiment, small amounts of impurities were found. At the same time, the surface fluctuation tended to influence the

experimental results. The calculated results might be useful for simplifying the tray simulation and evaluating the tray efficiency under different inclination.



(a) Flow of liquid and tilt of tray in the opposite direction



(b) Flow of liquid and tilt of tray in the same direction

Figure 10: Comparison of CFD simulations with experimental data and the Francis formula
($h_w=0.04 \text{ m}$, $\theta=2^\circ$)

CONCLUSIONS

A transient three-dimensional CFD model has been developed for simulating the liquid phase flow on a sieve tray under wind loads. The gas and liquid phases are modeled within the VOF framework. The predictions of the clear liquid height and liquid volume fraction from the CFD simulations show the right trend with varying liquid weir loads. The percentages of circulation area to total tray area along the z direction with varying inclination angle were obtained. Compared with the horizontal tray, the circulation area is bigger when the liquid flow and

the inclination of the tray are in the same direction, but when direction is the opposite, the circulation area is smaller. Moreover, it increases with increasing inclination angle when the direction of the liquid flow and inclination of tray are same. The circulation area is smaller when the direction is the opposite. There is an obvious enlargement of the fraction of the circulation area when the height is over the inlet in the z direction.

ACKNOWLEDGMENTS

This work was supported by the National Natural Science Foundation of China (Nos.21476142, 21306115 and 21106086), the Program for Liaoning Excellent Talents in University (No.LJQ2012035), the Science Foundation for doctorate Research of the Liaoning Science and Technology Bureau of China (No.20131090), the Science and Technology Research Project of Education Department of Liaoning province (No.L2013164).

NOMENCLATURE

C_μ, C_1, C_2	model constants	
E	Liquid expansion coefficient	
\mathbf{F}	body force	N/m^3
h_L	clear liquid height	m
h_w	weir height	m
k	turbulent kinetic energy	$\text{m}^2 \cdot \text{s}^{-2}$
l_w	length of the weir	m
N_{-x}	nodes of negative u_x in the z -plane	
N	the whole nodes in the z -plane	
p	pressure	Pa
Q_L	liquid loads	$\text{m}^3 \cdot \text{s}^{-1}$
t	time	s
u	velocity	$\text{m} \cdot \text{s}^{-1}$
x, y, z	coordinate	

Greek Letters

α	volume fraction of phase	$\text{m}^2 \cdot \text{s}^{-3}$
ε	turbulent dissipation	$\text{m}^2 \cdot \text{s}^{-3}$
μ	viscosity of phase	$\text{Pa} \cdot \text{s}$
μ_e	effective viscosity	$\text{m}^2 \cdot \text{s}^{-1}$
θ	inclination angle of tray	
ρ	density of phase	$\text{kg} \cdot \text{m}^{-3}$
$\sigma_k, \sigma_\varepsilon$	model constant	

Subscripts

- q* the qth phase
i, j co-ordinate index

REFERENCES

- Bell, R. L., Solari, R. B., Effect of Nonuniform velocity fields and retrograde flow on distillation tray efficiency. *AIChE Journal*, 20(4), 688-695 (1974).
- Buwa, V. V., Ranade, V. V., Dynamics of gas-liquid flow in a rectangular bubble column: Experiments and single/multi-group CFD simulations. *Chem. Eng. Sci.*, 57(22), 4715-4736 (2002).
- Chen, J. B., Liu, C. J., Yuan, X. G., CFD Simulation of flow and mass transfer in structured packing distillation columns. *Chinese Journal of Chemical Engineering*, 17(3), 381-388 (2009).
- Gesit, G., Nandakumar, K., Chuang, K. T., CFD modeling of flow and hydraulics of commercial-scale sieve trays. *AIChE Journal*, 49(4), 910-924 (2003).
- Hirt, C. W., Nichols, B. D., Volume of fluid (VOF) method for the dynamics of free boundaries. *Journal of Computational Physics*, 39(1), 201-225 (1981).
- Hong, R. Y., Numerical study of pinching liquid filament using VOF method. *Chinese Journal of Chemical Engineering*, 11(5), 542-549 (2003).
- Huang, J., Song, H.H., Liu, F. S., Liquid Channelling and its effect on plate efficiency. *Journal of Chemical Industry and Engineering*, 47(3), 311-315 (1996).
- Launder, B. E., 2nd-moment closure and its use in modeling turbulent industrial flows. *International Journal for Numerical Methods in Fluids*, 9(8), 963-985 (1989).
- Kister, H. Z., Larson, K. F., Madsen, P. E., Vapor cross flow channeling on sieve trays, fact or myth. *Chem. Eng. Prog.*, 88(11), 86-93 (1992).
- Krishna, R., Urseanu, M. I., Van Baten, J. M. and Ellenberger, J., Rise velocity of a swarm of large gas bubbles in liquids. *Chem. Eng. Sci.*, 54(2), 171-183 (1999).
- Krishna, R., Van Baten, J. M., Ellenberger, J., Higler, A. P., Taylor, R., CFD simulations of sieve tray hydrodynamics. *Chemical Engineering Research and Design*, 77(7), 639-646 (1999).
- Liu, B. T., Liu, C. J., Three dimensional simulation of liquid flow on distillation tray. *Chinese Journal of Chemical Engineering*, 10(5), 517-521 (2002).
- Liu, X. N., Lu, X. L., Effect of entrainment on tray efficiency of distillation columns. *Journal of Chemical Industry and Engineering*, 41(5), 762-767 (1990).
- Porter, K. E., Locket M. J., Lim C. T., The effect of liquid channeling on distillation plate efficiency. *Trans. Instn. Chem. Engr.*, 50(2), 91-101 (1972).
- Sun, Z. M., Liu, C. J., Yu, K. T., Yuan, X. G., Prediction of distillation column performance by computational mass transfer method. *Chinese Journal of Chemical Engineering*, 19(5), 833-844 (2011).
- Tao, W. Q., *Numerical Heat Transfer*. (2nd Ed.), Xi'an Jiao Tong University Press, 104-105 (2008).
- Van Baten, J. M., Krishna, R., Modelling sieve tray hydraulics using computational fluid dynamics. *Chemical Engineering Journal*, 77(3), 143-151 (2000).
- Wang, Y. L., Computational problems of clear liquid height on the weir. *Chemical World*, 2, 82-84 (1990).
- Yu, K. T., Yuan, X. G., You, X. Y., Liu, C. J., Computational fluid-dynamics and experimental verification of two-phase two-dimensional flow on a sieve column tray. *Chemical Engineering Research and Design*, 77(6), 554-560 (1999).
- Yu, K. T., Huang, J., Gu, F. Z., Simulation and efficiency of large tray (i)-eddy diffusion model with non-uniform liquid velocity field. *Chinese Journal of Chemical Engineering*, 2, 12-20 (1983).
- Zeng, A. W., Mal-distribution of weeping from a distillation tray and its effect on tray efficiency. *Chinese Journal of Chemical Engineering*, 10(5), 508-516 (2002).
- Zhang, P., Wang, C. H., Wu, J. H., Calculation of top deflection of tray column under working conditions. *Chemical Engineering*, 39(8), 37-39 (2011).
- Zhang, M. Q., Yu, K. T., Simulation of two dimensional liquid phase flow on a distillation tray. *Chin. J. Chem. Eng.*, 2(2), 63-71 (1994).